

The influence of Si delta doping on the electronic structure of AlGaAs-GaAs-AlGaAs single quantum wells

This article has been downloaded from IOPscience. Please scroll down to see the full text article.

1994 J. Phys.: Condens. Matter 6 4745

(<http://iopscience.iop.org/0953-8984/6/25/013>)

View [the table of contents for this issue](#), or go to the [journal homepage](#) for more

Download details:

IP Address: 171.66.16.147

The article was downloaded on 12/05/2010 at 18:42

Please note that [terms and conditions apply](#).

The influence of Si δ doping on the electronic structure of AlGaAs–GaAs–AlGaAs single quantum wells

W Xu and J Mahanty

Department of Theoretical Physics, Research School of Physical Sciences and Engineering,
The Australian National University, Canberra, ACT 0200, Australia

Received 11 November 1993, in final form 5 April 1994

Abstract. The subband structure of a two-dimensional electron gas (2DEG) in an Si δ -doped Al_cGa_{1-c}As–GaAs–Al_cGa_{1-c}As single quantum well is calculated in the envelope function approach at zero temperature. A model is developed in which the confinement potential energy, the subband energies and wavefunctions, the total electron density and the electron density in the different electronic subbands and the depletion lengths can be calculated as functions of known material properties and growth parameters only. A detailed theoretical study of the influence of Si δ doping in the GaAs layer on the electronic structure is presented for single quantum wells. The conditions which have to be satisfied to form a 2DEG in the structure are obtained analytically. The main effect of the presence of an Si δ -doped layer in GaAs on the electronic structure of the quantum well results from an extra confinement potential and from the smaller depletion lengths in the modulation-doped AlGaAs layers.

1. Introduction

Over the last two decades techniques such as MBE and MOCVD have made it possible to grow alternately atomically smooth layers of different semiconductors such as two-dimensional (2D) electron systems. Together with modulation doping techniques these structures have very interesting and important properties both for device applications (HEMT [1] and quantum well laser [2], etc) and for observations of new 2D effects (quantum Hall effects [3], electro-phonon resonance effects [4], etc). One of the central problems in designing and applying these 2D semiconductor devices is the determination of the electronic subband structure which plays an essential role in determining almost all physically measurable properties. Experimental measurements, such as of Shubnikov–de Haas oscillations, Hall effects, photoluminescence and photoluminescence excitation are often used to determine the electronic states of 2D systems. Theoretically self-consistent calculations such as those proposed by Ando [5] and Stern and Das Sarma [6] provide powerful tools in calculating the electronic structure of 2D semiconductor systems such as heterojunctions [5–8], δ -doped layers [9], single quantum wells [10–13], and recently, parabolic quantum wells [14]. In 1985 Hurkx and van Haeringen [8] proposed a theoretical model to determine the electronic structure in a selectively doped AlGaAs/GaAs heterostructure. The main merits of this model are that the electronic states can be calculated by taking into account the known material properties and the sample growth parameters only and that the effect of depletion is included. This model has been successfully applied to calculations in heterojunctions [8] and single quantum wells [13].

In this paper we present a detailed self-consistent calculation on the Al_cGa_{1-c}As–GaAs–Al_cGa_{1-c}As (with c being the aluminium content) single-quantum-well (SQW) systems in

the cases with and without Si δ doping in the middle of the quantum well (QW) layer. The selectively doped AlGaAs–GaAs–AlGaAs SQW systems have been an important category of 2D electron structures, due to their potential application to, e.g., SQWT [12] and FET [15] devices. In practical applications of these electronic devices it is desirable to have large electron densities in order for example to minimize the resistance. A possible way to generate a larger electron density in a SQW system is to dope Si in the well layer [16]. Doped Si in the GaAs layer will play the role of donor. With present day techniques it is possible to control the concentration and doping profile and to obtain a doping profile with a very narrow thickness (so called δ doping). The electronic properties in Si δ -doped SQW systems have recently received attention [17]. For the above-mentioned applications and for guidance in design of devices it would be valuable to calculate, for instance, the electron density, the energies, and the wavefunctions of the electronic subbands, and electron distribution along the direction of the confinement potential as well as the depletion lengths from growth parameters (concentrations of the donor and acceptor dopants, spacer distances, Al content, concentration and thickness of the δ -doped layer, width of the quantum well layer, etc) and from material properties (effective masses, conduction band discontinuity, donor binding energy, etc). Furthermore it would be valuable to look into the influence of the δ doping in the well layer on the electronic structure of the SQW, and this is the motivation of our present study. In this paper we generalize the model proposed by Hurkx and van Haeringen in [8] to the selectively doped AlGaAs–GaAs–AlGaAs single-quantum-well systems in the cases with and without δ doping in the GaAs layer. The method of our self-consistent calculation is described in section 2. The numerical results are presented and discussed in section 3 and the conclusions are summarized in Sec. 4.

2. Outline of the model and the calculation

The present paper describes a self-consistent calculation on a single quantum well which consists of a GaAs layer (with a width L) adjacent to two $\text{Al}_c\text{Ga}_{1-c}\text{As}$ layers; an Si δ -doped layer (with a thickness W_d) is located in the middle of the GaAs layer. The sample structure is depicted in figure 1. For the model calculation we consider the following conditions.

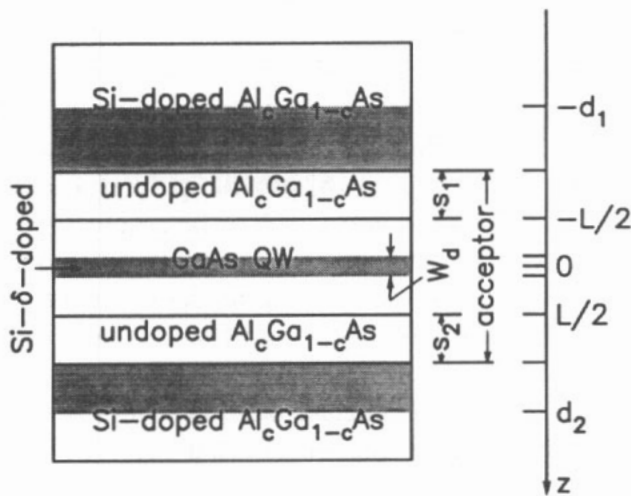


Figure 1. Schematic diagram of an Si δ -doped $\text{Al}_c\text{Ga}_{1-c}\text{As}$ –GaAs– $\text{Al}_c\text{Ga}_{1-c}\text{As}$ single quantum well. c is the aluminium content, W_d the thickness of the δ -doped layer, L the width of the quantum well, s_1 and s_2 are the spacer distances, and d_1 and d_2 are the depletion lengths.

(1) The AlGaAs layers are uniformly doped with Si with the concentration N_s except for the (spacer) layers of widths s_1 and s_2 , respectively, measured from the interfaces between GaAs and AlGaAs. These modulation-doped Si in AlGaAs will play the role of donors. These donor levels are all supposed to lie at an energy E_d (donor binding energy) below the conduction band edge of AlGaAs.

(2) The modulation-doped Si in the two AlGaAs regions are not completely ionized. By taking the depletion effect into consideration we suppose that the doped Si are only ionized within the (shaded) regimes $-d_1 < z < -s_1 - L/2$ and $s_2 + L/2 < z < d_2$, respectively. The depletion lengths d_1 and d_2 will be determined in the following self-consistent calculations.

(3) The GaAs layer along with the Si-undoped AlGaAs spacer layers is slightly and uniformly doped with acceptors with the concentration N_a . For a sample without heavy acceptor doping and with a relatively thin GaAs layer, we may assume that all the acceptors are ionized and may neglect the influences of both the acceptor levels and the band gap in the GaAs. For a high-quality sample the acceptor concentration is very small in comparison with the doped donor concentration; we may neglect the influence of acceptors in the Si-doped AlGaAs regimes and in the δ -doped GaAs regime.

(4) In the δ -doped layer when the concentration of doped Si (N_d) is below the saturation, i.e., $N_d < 4 \times 10^{25} \text{ m}^{-3}$, we assume that all the δ -doped donors are ionized and uniformly distributed within the regime of W_d for the sake of simplicity. We neglect the diffusion of δ -doped Si in GaAs.

(5) Due to thermodynamic equilibrium the Fermi energy E_F is constant across the device. As pointed out in [8] and [13] at $T = 0 \text{ K}$ and for a donor-doped 2D semiconductor system E_F can be taken as the highest populated level which is the donor level E_d in AlGaAs, i.e., $E_F = E_d$. This assumption is based on the thermodynamic statistics in impurity semiconductors [18].

In general the electronic states for the two-dimensional electron gas (2DEG), such as that realized in δ -doped SQW systems discussed in this paper, are described by the Schrödinger equation for the eigenfunction and eigenvalue and by the Poisson equation for the confinement potential. These have to be solved together self-consistently. To simplify matters we assume, in accordance with the above-quoted references [5–14], the confinement potential energy seen by electrons depends only on the coordinate z perpendicular to the interfaces. Applying the envelope function approach to the effective-mass formalism leads to envelope functions of the kind $\Psi(\mathbf{R}) = e^{i\mathbf{k}\cdot\mathbf{r}}\psi_n(z)$ with the corresponding energy spectrum of the electron $E_n(\mathbf{k}) = E(\mathbf{k}) + \varepsilon_n$, where $\mathbf{R} = (\mathbf{r}, z) = (x, y, z)$, $\mathbf{k} = (k_x, k_y)$. Further, when the parabolic band structure is considered, $E(\mathbf{k}) = \hbar^2 k^2 / 2m^*$ is the kinetic energy for free electron motion in the xy plane with m^* the effective electron mass. Here the electron wavefunctions along the z direction $\psi_n(z)$ and the electronic subband energies ε_n for a δ -doped $\text{Al}_c\text{Ga}_{1-c}\text{As}$ –GaAs– $\text{Al}_c\text{Ga}_{1-c}\text{As}$ SQW are determined by the one-dimensional Schrödinger equation

$$\left[-\frac{\hbar^2}{2} \frac{d}{dz} \frac{1}{m^*(z)} \frac{d}{dz} + U(z) - \varepsilon_n \right] \psi_n(z) = 0 \quad (1)$$

where for $\text{Al}_c\text{Ga}_{1-c}\text{As}$ /GaAs systems the effective electron mass ratio can be obtained by [19]

$$\frac{m^*(z)}{m_e} = \begin{cases} m_0^*/m_e & |z| < L/2 \\ m_0^*/m_e + 0.088c & \text{otherwise} \end{cases} \quad (2)$$

with m_e the electron rest mass and m_0^* the effective electron mass for GaAs, i.e., for $c = 0$. The confinement potential energy in equation (1) is given by

$$U(z) = U_c(z) + U_{xc}(z) + \Delta E_c(z) \quad (3)$$

where $\Delta E_c(z)$ is the conduction band edge discontinuity; in the well (i.e., in GaAs) $\Delta E_c(z) = 0$ and in the barrier (i.e., in $\text{Al}_c\text{Ga}_{1-c}\text{As}$) $\Delta E_c(z) = U_0$ which can be calculated by [19]

$$U_0 \simeq 0.6(1.155c + 0.37c^2) \quad (\text{in eV}). \quad (4)$$

Further, $U_{xc}(z) = -e\varphi_{xc}(z)$, with the electron charge $-e$ and the potential $\varphi_{xc}(z)$, results from the exchange and correlation effects in the density-functional theory (DFT) [20, 21], and $U_c(z) = -e\varphi_c(z)$, with $\varphi_c(z)$ the Hartree potential, is the Coulomb interaction term resulting from charge interaction and can be determined by the Poisson equation

$$-e \frac{d^2\varphi_c(z)}{dz^2} = \frac{d^2U_c(z)}{dz^2} = \frac{e\rho(z)}{\kappa} \quad (5)$$

with $\rho(z)$ the charge density and κ the dielectric constant of the material. In this paper we ignore the difference in κ between the two materials GaAs and AlGaAs because of the relatively weak effect [13] and we assume an isotropic κ in the sample system.

In general the exchange–correlation potential energy is an unknown functional $U_{xc}(z) = U_{xc}[n(z)]$ of the electron density $n(z)$. In the practical calculations one is often forced to take some simple approximations to obtain the functional form of $U_{xc}[n(z)]$. One of the simplest and most popularly used approximations is the local-density approximation (LDA) [22] which has been successfully applied to calculate the 2D electronic structures of heterojunctions [6], SQW structures [11], and parabolic quantum wells [14]. In this paper an analytic form proposed by Hedin and Lundqvist [23] is used for calculating $U_{xc}(z)$ through

$$U_{xc}(z) = U_{xc}[n(z)] = -[1 + 0.7734y \ln(1 + y^{-1})] \frac{2R_y^*}{\pi\alpha r_s} \quad (6)$$

where $\alpha = (4/9\pi)^{1/3}$, $y = y(z) = r_s/21$, the effective Rydberg constant is given by $R_y^* = e^2/(8\pi\kappa a^*)$ with the effective Bohr radius $a^* = 4\pi\kappa\hbar^2/[e^2m^*(z)]$, and the parameter r_s is defined by

$$r_s = r_s[n(z)] = \left[\frac{4\pi a^{*3} n(z)}{3} \right]^{-1/3}.$$

In SQW structures the potential energy $U_{xc}(z)$ may be discontinuous at the interfaces between GaAs and AlGaAs (i.e. at $z = \pm L/2$) because of different effective electron masses.

For the δ -doped AlGaAs–GaAs–AlGaAs single quantum well depicted by figure 1, if N_d is the δ -doped donor concentration, N_s is the modulation-doped donor concentration and N_a is the acceptor concentration, the functional form of the charge density $\rho(z)$ can be modelled by

$$\rho(z) = -e \begin{cases} n(z) & z < -d_1 \\ n(z) - N_s & -d_1 < z < -L/2 - s_1 \\ n(z) + N_a & -L/2 - s_1 < z < -W_d/2 \\ n(z) - N_d & -W_d/2 < z < W_d/2 \\ n(z) + N_a & W_d/2 < z < L/2 + s_2 \\ n(z) - N_s & L/2 + s_2 < z < d_2 \\ n(z) & z > d_2 \end{cases} \quad (7)$$

where a conventional SQW structure (without δ doping in the GaAs regime) can be obtained by taking $W_d \rightarrow 0$ and $N_d \rightarrow 0$. We note that the present calculation on the conventional SQW systems goes beyond the work by [13] through considering (1) the different effective electron masses in AlGaAs and GaAs and (2) the effect of asymmetric modulation doping, i.e., possibly $s_1 \neq s_2$. At $T = 0$ K and referring the energy to the minimum of the conduction band edge in the well, the electron density along the z -direction is given by

$$n(z) = \frac{m_0^*}{\pi \hbar^2} \sum_n (E_F - \varepsilon_n) |\psi_n(z)|^2 \Theta(E_F - \varepsilon_n) \quad (8)$$

with $\Theta(x) = 0$ ($x < 0$), 1 ($x \geq 0$) the unit-step function. Here we have used the definition of the density of states (DOS) for a 2DEG

$$D(E) = \frac{m_0^*}{\pi \hbar^2} \sum_n \Theta(E - \varepsilon_n) \quad (9)$$

from which we can also calculate the sheet electron density in different electronic subbands and the total electron density per unit area, respectively, through

$$N_n = \frac{m_0^*}{\pi \hbar^2} (E_F - \varepsilon_n) \Theta(E_F - \varepsilon_n) \quad N_T = \sum_n N_n. \quad (10)$$

In the above we have used the effective electron mass of the well layer as the representative density of states effective mass. As pointed out by [13] the sheet electron density depends very little on the temperature up to 100 K; our theoretical results obtained from zero-temperature calculations may be compared with the experimental data obtained at non-zero temperatures.

To solve equation (5) with the charge distribution given by equation (7), we need to define the boundary conditions. Since the confinement potential energy in the regimes outside the depletion lengths ($z < -d_1$ and $z > d_2$) depends very little on the distance we can integrate both Schrödinger and Poisson equations from $-\infty$ to $+\infty$ along the z axis. By following what was proposed by [8] and by assuming that the Fermi level of the whole SQW structure is identified with the donor level at $T = 0$ K, at $z \rightarrow \pm\infty$ we have $U(\pm\infty) = E_d$. Furthermore, the nature of $\psi_n(\pm\infty) = 0$ for the eigenfunctions, taking into account the depletion effect, leads to the following boundary conditions:

$$U_c(\pm\infty) = E_d - U_0 \quad \left. \frac{dU_c(z)}{dz} \right|_{z \rightarrow \pm\infty} = 0. \quad (11)$$

Using the above boundary conditions and using the continuities of $U_c(z)$ and $dU_c(z)/dz$, after integrating equation (5) twice we obtain

$$U_c(z) = \begin{cases} U_L(z) & z \leq -d_1 \\ U_L(z) - DN_s(z + d_1)^2/2 & -d_1 \leq z \leq -L/2 - s_1 \\ U_L(z) - DN_s(d_1 - L/2 - s_1)(d_1 + L/2 + s_1 + 2z)/2 \\ \quad + DN_a(L/2 + s_1 + z)^2/2 & -L/2 - s_1 \leq z \leq -W_d/2 \\ U_L(z) - DN_s(d_1 - L/2 - s_1)(d_1 + L/2 + s_1 + 2z)/2 \\ \quad + DN_a(L/2 + s_1 - W_d/2)(L/2 + s_1 + W_d/2 + 2z) \\ \quad - DN_d(W_d/2 + z)^2/2 & -W_d/2 \leq z \leq 0 \\ U_R(z) - DN_s(d_2 - L/2 - s_2)(d_2 + L/2 + s_2 - 2z)/2 \\ \quad + DN_a(L/2 + s_2 - W_d/2)(L/2 + s_2 + W_d/2 - 2z) \\ \quad - DN_d(W_d/2 - z)^2/2 & 0 \leq z \leq W_d/2 \\ U_R(z) - DN_s(d_2 - L/2 - s_2)(d_2 + L/2 + s_2 - 2z)/2 \\ \quad + DN_a(L/2 + s_2 - z)^2/2 & W_d/2 \leq z \leq L/2 + s_2 \\ U_R(z) - DN_s(z - d_2)^2/2 & L/2 + s_2 \leq z \leq d_2 \\ U_R(z) & z \geq d_2 \end{cases} \quad (12)$$

where $D = -e^2/\kappa$, $U_L(z) = E_d - U_0 + Dg(z)$ and $U_R(z) = E_d - U_0 + Dh(z)$ are the potential energies induced by electron distribution, i.e., $d^2U_L(z)/dz^2 = d^2U_R(z)/dz^2 = Dn(z)$, and $g(z)$ and $h(z)$ are given, respectively, by

$$g(z) = \int_{-\infty}^z dz_1 \int_{-\infty}^{z_1} dz_2 n(z_2) \quad h(z) = \int_{+\infty}^z dz_1 \int_{+\infty}^{z_1} dz_2 n(z_2).$$

The continuities of $dU_c(z)/dz$ and $U_c(z)$ at $z = 0$ lead to, respectively,

$$N_T = \int_{-\infty}^{\infty} dz n(z) = N_d W_d + N_s(d_1 + d_2 - L - s_1 - s_2) - N_a(L + s_1 + s_2 - W_d) \quad (13a)$$

which can also be obtained from the Gauss law and from the charge neutrality condition, and

$$d_1^2 - d_2^2 = \left(1 + \frac{N_a}{N_s}\right)(s_1 - s_2)(L + s_1 + s_2) + \frac{2}{N_s}[g(0) - h(0)]. \quad (13b)$$

For symmetric modulation doping, i.e., for $s_1 = s_2$, equation (13b) leads to $d_1 = d_2$. $d_1 \neq d_2$ for asymmetric doping $s_1 \neq s_2$. By solving equations (13) we can determine the depletion lengths d_1 and d_2 which make $dU_c(z)/dz$ and $U_c(z)$ continuous along the z direction. When the solutions satisfy $d_1 > L/2 + s_1$ and $d_2 > L/2 + s_2$ (i.e., there are some ionized donors in the modulation-doped AlGaAs layers) along with $N_T > 0$ (i.e., the 2DEG is formed), the chosen growth parameters, such as the spacers (s_1 and s_2), the width of well (L), the width of δ doping (W_d), and the doped donor and acceptor concentrations (N_d , N_s , and N_a), lead to the formation of a 2DEG in the quantum well. Namely, equations (13) give the conditions which have to be satisfied to obtain the 2DEG in a δ -doped SQW structure. This would be helpful to guide device design. In this paper we deal with the situation where there are ionized donors in the doped AlGaAs regimes. Our model calculation shown above is invalid in the case where the selectively doped donors in AlGaAs layers are not ionized at all ($d_i < L/2 + s_i$, $i = 1, 2$) or in the case without modulation doping in AlGaAs.

3. Numerical results and discussions

In this paper our calculations are performed for AlGaAs–GaAs–AlGaAs single quantum wells by taking the following material parameters: (i) the effective mass of GaAs $m_0^* = 0.0665m_e$ and (ii) the dielectric constant of GaAs $\kappa = 12.9$. For donors induced by doping Si in the AlGaAs region the donor binding energy E_d is taken as a typical value [13] $E_d = 96$ meV. The growth parameters can be taken from the experimental data. In all calculations we use a typical acceptor concentration $N_a = 2 \times 10^{20} \text{ m}^{-3}$ and we use Al content $c = 30\%$ which leads to a conduction band discontinuity $U_0 \simeq 227$ meV at the interface between $\text{Al}_c\text{Ga}_{1-c}\text{As}$ and GaAs and to an effective electron mass $m^* \simeq 0.0929m_e$ in AlGaAs layers, according to equations (4) and (2), respectively.

Applying the ‘turning point’ technique to the Numerov algorithm [24], the Schrödinger equation can be solved by using the boundary conditions $\psi_n(\pm\infty) = 0$. We find this technique is very suitable for solving Schrödinger equations with different effective masses. The Poisson equation is solved by an iteration technique. In our self-consistent calculations, the iteration is interrupted when $\max|U_{j+1}(z) - U_j(z)|$, i.e., the maximum difference of the total confinement potential energy between two successive iteration steps j and $j + 1$, is smaller than 0.1 meV.

The numerical results of the total confinement potential energy and the electron density as a function of the distance along the direction perpendicular to the interfaces of an SQW are shown in figure 2 ($L = 8 \text{ nm} = 80 \text{ \AA}$) and figure 3 ($L = 14 \text{ nm} = 140 \text{ \AA}$) in the situation with (solid curves) and without (dotted curves) δ doping in the well layer at fixed spacers $s_1 = s_2$ and donor and acceptor concentrations. In figures 2 and 3 the energies of the different electronic subbands are also shown for the cases with and without δ doping. The dashed curves, obtained from the difference between the total confinement potential energy in the case with δ doping (solid curves) and in the case without δ doping (dotted curves), show the net influence of the δ doping on the total confinement potential energy. The presence of the δ -doped layer will (i) lower the total confinement potential referred to the Fermi level and (ii) enhance the separation between occupied electronic subbands and Fermi level, and consequently a larger electron density can be obtained in the δ -doped structures. From figures 2 and 3 it can be seen that the influence of the δ doping on the electronic states of the SQW results from (i) an extra confinement potential (dashed curves in figures 2 and 3) which is caused mainly by the Coulomb interaction of the ionized donors in the δ -doped layer and (ii) smaller depletion lengths (see the captions of figures 2 and 3) in the selectively doped AlGaAs regimes. It is interesting to note that with the δ -doping technique one can obtain a *rectangular* profile of the confinement potential energy (see figures 2 and 4). The influence of the δ -doped donor concentration on the confinement potential energy is shown in figure 4. The net potential energy induced by the δ doping (see figure 4(b)) increases with increasing doping concentration. The asymmetric structure of the potential profiles is caused by the asymmetric modulation doping $s_1 \neq s_2$. Our numerical results presented in figures 2–4 show that the presence of a δ -doped layer in the middle of the quantum well can vary markedly the total confinement potential both in position referred to the Fermi level and in its profile. In figure 4(b) the maximum potential energy caused by δ doping can be observed up to 36 meV in comparison with the conduction band edge discontinuity $U_0 \simeq 227$ meV at $c = 0.3$.

The dependence of the electronic structure on the width of the quantum well is presented in figure 5 where we plot (a) the total electron density per unit area N_T and the electron density for the occupied electric subband N_n , (b) the energies for the different subbands ε_n and the Fermi energy E_F and (c) the depletion lengths as a function of the width of the

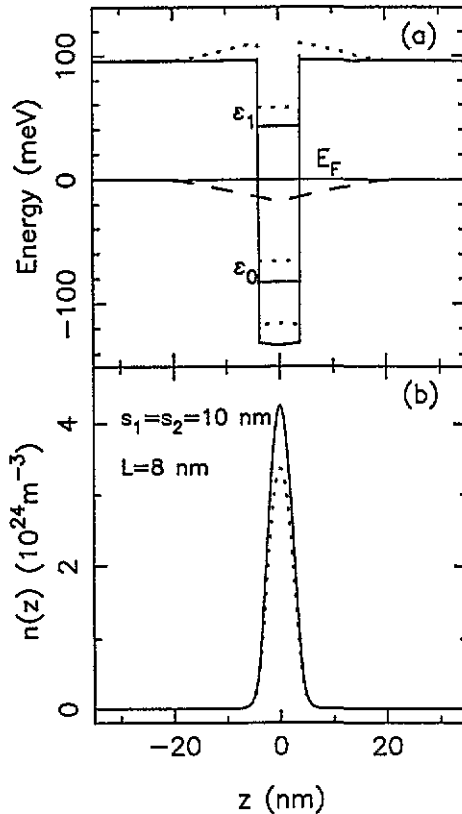


Figure 2. (a) The confinement potential energy and (b) the electron density as a function of the distance along the z axis for the sample with (solid curves) and without (dotted curves) δ doping in the well layer. The dashed curve in (a) is the net confinement potential induced by δ doping. E_F is the Fermi energy (thinner solid curve) and ϵ_n is the energy level for the n th electronic subband. For the width of well layer $L = 8$ nm only the lowest subband is occupied by electrons. The spacers $s_1 = s_2$ result in the depletion lengths $d_1 = d_2$. The modulation-doped donor concentration $N_s = 10^{24} \text{ m}^{-3}$ and acceptor concentration $N_a = 2 \times 10^{20} \text{ m}^{-3}$. The concentration and thickness of the δ -doped layer are $N_d = 7 \times 10^{24} \text{ m}^{-3}$ and $W_d = 3$ nm, respectively. For the sample with (without) δ doping, the sheet electron density $N_T = N_0 = 2.30 \times 10^{16} \text{ m}^{-2}$ ($1.84 \times 10^{16} \text{ m}^{-2}$) and the depletion lengths in the doped AlGaAs layers $d_1 - s_1 - L/2 = d_2 - s_2 - L/2 = 0.99$ nm (9.18 nm).

quantum well L for fixed spacers, donor density N_s and acceptor density N_a . The solid (dashed) curves are for the sample with (without) δ doping. With increasing width of the quantum well (1) the total electron density increases, (2) the excited states are occupied by electrons, (3) the Fermi energy and the electronic subband energies (measured from the minimum of the conduction band edge in the GaAs layer for the δ -doped system (solid curves) and from the potential energy close to the interface in the GaAs regime for the SQW without δ doping (dashed curves)) decrease and (4) the depletion lengths increase. The longer depletion lengths imply that more donors in the AlGaAs regimes are ionized, which leads to the increase of the total electron density. Figure 5 shows that the electronic structures of the SQW in the cases with and without δ doping have a similar dependence on the width of the quantum well except for which the larger electron densities and the smaller depletion lengths can be observed in the presence of the δ -doped layer.

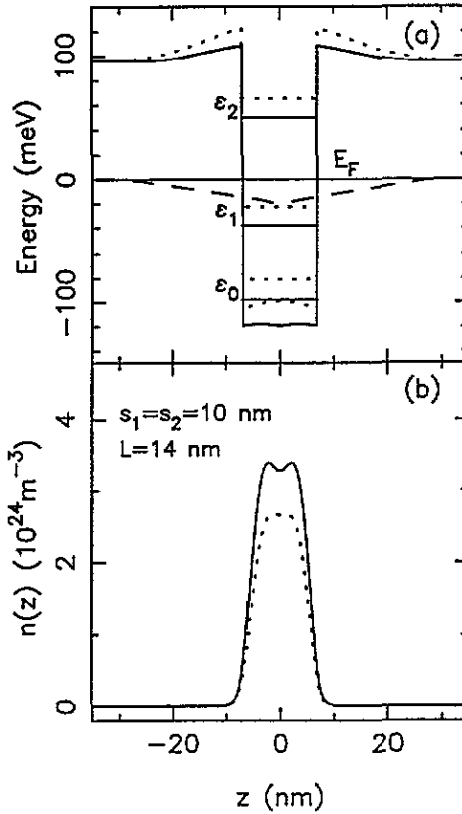


Figure 3. The confinement potential energy and the electron density as a function of the distance in the z direction. The lines and the parameters are same as in figure 2 except for taking $L = 14$ nm which leads to two-subband occupancy. For the sample with (without) δ doping, $N_T = 3.78 \times 10^{16} \text{ m}^{-2}$ ($2.84 \times 10^{16} \text{ m}^{-2}$), $N_0 = 2.72 \times 10^{16} \text{ m}^{-2}$ ($2.22 \times 10^{16} \text{ m}^{-2}$), $N_1 = 1.06 \times 10^{16} \text{ m}^{-2}$ ($6.20 \times 10^{15} \text{ m}^{-2}$) and $d_1 - s_1 - L/2 = d_2 - s_2 - L/2 = 8.38$ nm (14.18 nm).

The dependences of the electron densities, the electronic subband energies, the Fermi energy and the depletion lengths on the thickness and concentration of the Si δ -doped layer in GaAs are shown in figures 6 and 7, respectively, for fixed quantum well width, spacers, modulation-doped donor concentration and acceptor concentration. $W_d = 0$ and/or $N_d = 0$ correspond to the situation without δ doping in the well layer. Increasing W_d and/or N_d leads to an increase in the ionized donors (note we have assumed that all the δ -doped donors are ionized) and consequently to an increase in the electron densities. In an SQW system, the electronic subband energies are mainly determined by the width of the quantum well and therefore depend weakly on the δ doping. With increasing W_d and/or N_d the self-consistency between the total electron density and the energies of the electronic subband results in an increase of the Fermi energy and in a decrease of the depletion lengths in the doped AlGaAs regimes, which lead to a non-linear increase of the total electron density with W_d and N_d .

In the presence and absence of the δ -doped layer in the middle of the quantum well the total electron density, the electron densities for occupied subbands, the Fermi energy, the subband energies and the depletion lengths as functions of modulation-doped donor concentration are shown in figure 8. Increasing donor concentration N_s in the doped AlGaAs

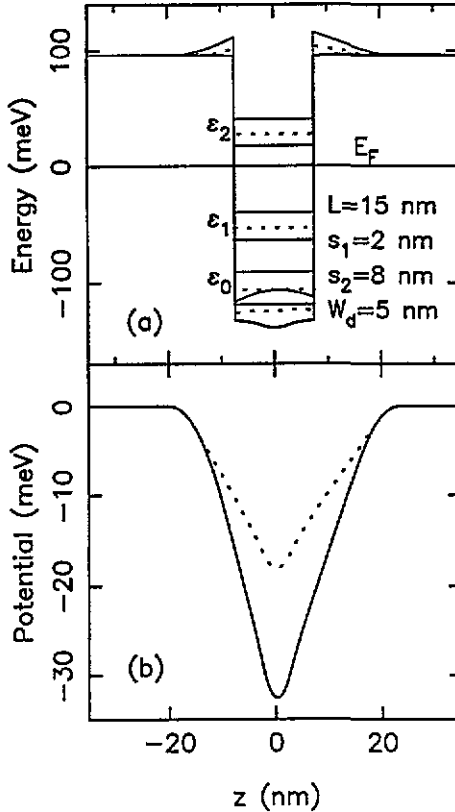


Figure 4. (a) The total confinement potential energy and (b) the net confinement potential energy induced by δ doping as a function of the distance along the z axis for different δ doping conditions: $N_d = 0$ (thinner solid curve), $5 \times 10^{24} \text{ m}^{-3}$ (dotted curves) and 10^{25} m^{-3} (thick solid curves). $N_s = 2 \times 10^{24} \text{ m}^{-3}$ and $N_a = 2 \times 10^{20} \text{ m}^{-3}$. The asymmetric structure of the potential energies is caused by asymmetric modulation doping $s_1 \neq s_2$.

regimes leads firstly to an increase in the electron densities and then to the saturation of the total electron density because of decreasing depletion lengths. This process implies that the total number of ionized donors in the sample system increases and then becomes roughly constant. For samples where $N_a \ll N_s$, the total number of ionized donors is given by $N_T - N_d W_d$, with N_T , N_d and W_d being constants, according to equation (13a). For such a large N_s that the depletion length $d_i - L/2 - s_i < 1 \text{ nm}$ ($i = 1, 2$) is reached, which is the case for $N_s > 2 \times 10^{25} \text{ m}^{-3}$ in figure 8, the theoretical results are not very reliable because now (a) the depletion length is of the order of the lattice constant which is $a \sim 0.6 \text{ nm}$ for AlGaAs (small values of the depletion length are not accurate for a real experimental device), (b) the distance between donors in AlGaAs becomes large (e.g., for $N_s = 2 \times 10^{25} \text{ m}^{-3}$ this distance is about 3.7 nm) compared to the depletion lengths and (c) impurity conduction in the AlGaAs layers may occur in the sample and normally can be observed by parallel conductance experimentally.

The influence of the spacer distance on the electronic structure of the SQW systems in the presence and absence of a δ -doped layer is shown in figure 9 and figure 10 where we plot the electron densities, the Fermi energy, the energies of the electronic subbands, and the depletion lengths as functions of spacer distance in the cases of symmetric (figure

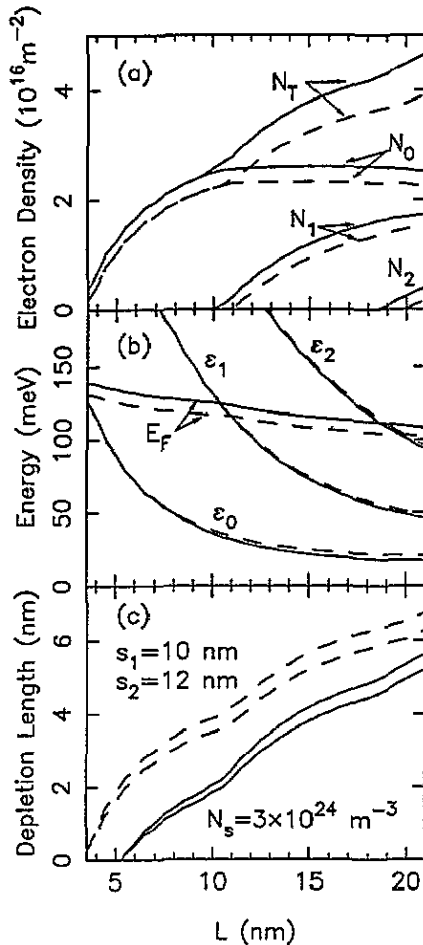


Figure 5. (a) N_T and N_n , (b) ϵ_n and E_F measured from the minimum of the conduction band edge in the GaAs layer for the δ -doped sqw and from $U(-L/2 + 0)$ (note $U(-L/2 + 0) < U(L/2 - 0)$ when $s_1 < s_2$) the potential energy close to the interface in the GaAs regime for the sqw without δ doping, respectively, and (c) the depletion lengths $d_1 - s_1 - L/2$ and $d_2 - s_2 - L/2$ as a functions of the width of the quantum well. The solid (dashed) curves are for the sample with (without) δ doping. $N_d = 2 \times 10^{20} \text{ m}^{-3}$. For the δ -doped layer $N_d = 7 \times 10^{24} \text{ m}^{-3}$ and $W_d = 2 \text{ nm}$. In (c) the difference between $d_1 - s_1 - L/2$ (upper curve) and $d_2 - s_2 - L/2$ (lower curve) is induced by the asymmetric modulation doping.

9, $N_s = 10^{24} \text{ m}^{-3}$) and asymmetric (figure 10, $N_s = 2 \times 10^{24} \text{ m}^{-3}$ and $s_1 = 10 \text{ nm}$ is fixed) modulation doping in the AlGaAs regimes. For the symmetric doping ($s_1 = s_2$) figure 9 shows that the electron densities decrease with increasing spacers because of the decreasing depletion lengths. In figure 10 we fix the spacer s_1 (in the upper doped AlGaAs regime in figure 1) and vary the spacer s_2 (in the lower doped AlGaAs regime in figure 1). With increasing s_2 the depletion length in the upper (lower) AlGaAs layer increases (decreases) and the total electron density decreases. The nearly identical natures shown in (a) and (b) in figures 9 and 10 imply that (i) the effects caused by different doping appear to compensate and (ii) asymmetric modulation doping has a weak influence on the electronic structure. However, the marked difference in the depletion layers between symmetric and

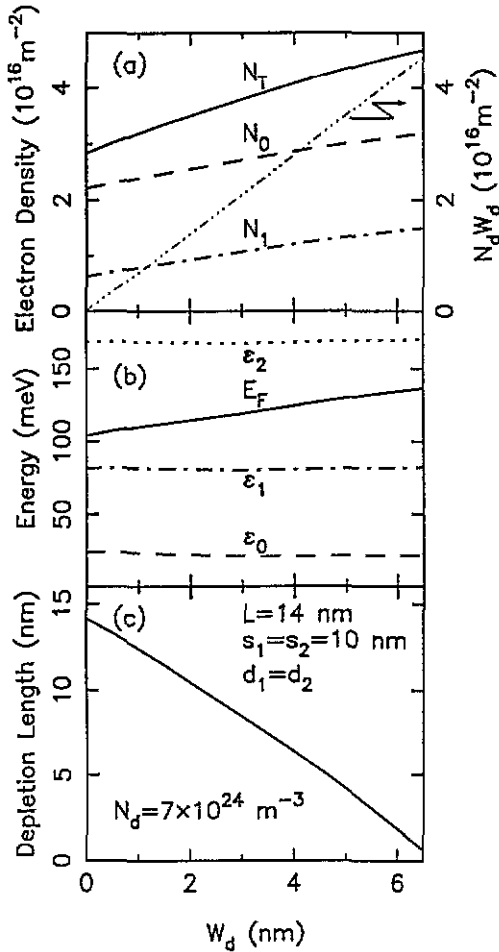


Figure 6. (a) N_T and N_n , (b) E_F and ϵ_n and (c) the depletion lengths as functions of the thickness of the δ -doped layer for a fixed N_d . In the calculations $N_s = 10^{24} \text{ m}^{-3}$ and $N_a = 2 \times 10^{20} \text{ m}^{-3}$ are used. $s_1 = s_2$ results in $d_1 = d_2$. $W_d = 0$ corresponds to the case without a δ -doped layer in the well. In (a) the thinner curve shows the variation of $N_d W_d$.

asymmetric systems (see figures 9(c) and 10(c)) may lead to different electronic properties, e.g., to different electronic mobility. From figures 9 and 10 it can also be seen that (i) the electronic subband energies depend very little on the spacer distances and (ii) the Fermi energy decreases slowly with increasing spacer distance.

Our numerical results show that the inclusion of the different effective electron masses in two materials GaAs and $\text{Al}_c\text{Ga}_{1-c}\text{As}$ leads to a slightly smaller (about 3%) total electron density than that obtained by taking $m^*(z) = m_0^*$. As an important improvement in the present paper we have included the effect of depletion on the electronic structure of SQW samples. In our model calculations, the 2DEG will not be formed (i.e., $N_T > 0$ cannot be achieved) in the SQW samples in the cases of a small depletion length ($d_i < L/2 + s_i$, $i = 1$ and/or 2), which corresponds to a heavy δ doping. When such a heavy Si δ doping in the GaAs layer is achieved that $N_d W_d > N_T$ and consequently $d_1 + d_2 - L - s_1 - s_2 < 0$ (obtained from equation (13a)), doped donors in the AlGaAs layers are not ionized at all.

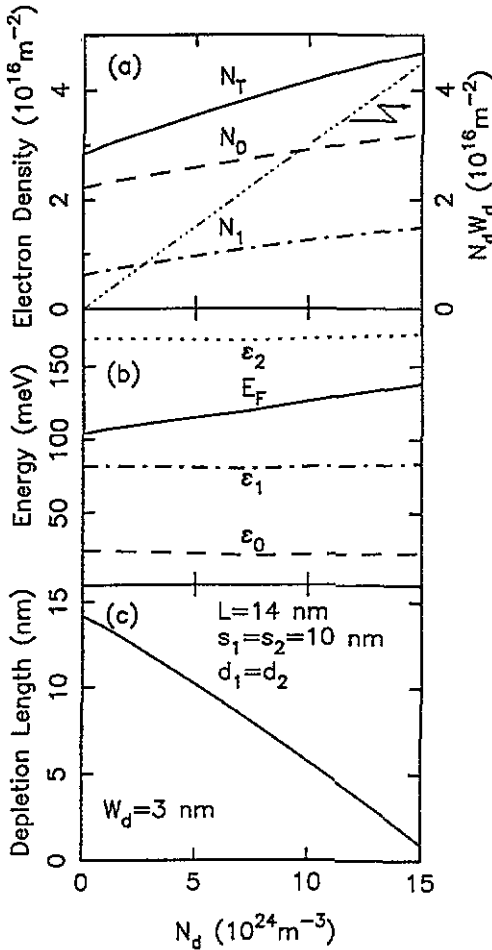


Figure 7. The electronic properties of the δ -doped sqw as functions of the concentration of the δ -doped layer for a fixed W_d . In (a) the thinner curve shows the variation of $N_d W_d$. The other lines and parameters are the same as in figure 6. $N_d = 0$ corresponds to the case of no δ -doped layer in the quantum well.

In this case the depletion layers are replaced by accumulation layers, which cannot be dealt with by our present model.

The depletion lengths in the structure can provide the information about the impurity distributions in a δ -doped SQW sample, which is of importance to the calculation of, for example, the mobility limited by impurity scattering. For the sample depicted in figure 1 we can model the impurity distribution as

$$n_i(z) = \begin{cases} N_s & -d_1 < z < -L/2 - s_1 & L/2 + s_2 < z < d_2 \\ N_a & -L/2 - s_1 < z < -W_d/2 & W_d/2 < z < L/2 + s_2 \\ N_d & -W_d/2 < z < W_d/2. \end{cases} \quad (14)$$

Thus we can calculate the low-temperature mobility by taking the known material properties and growth parameters only.

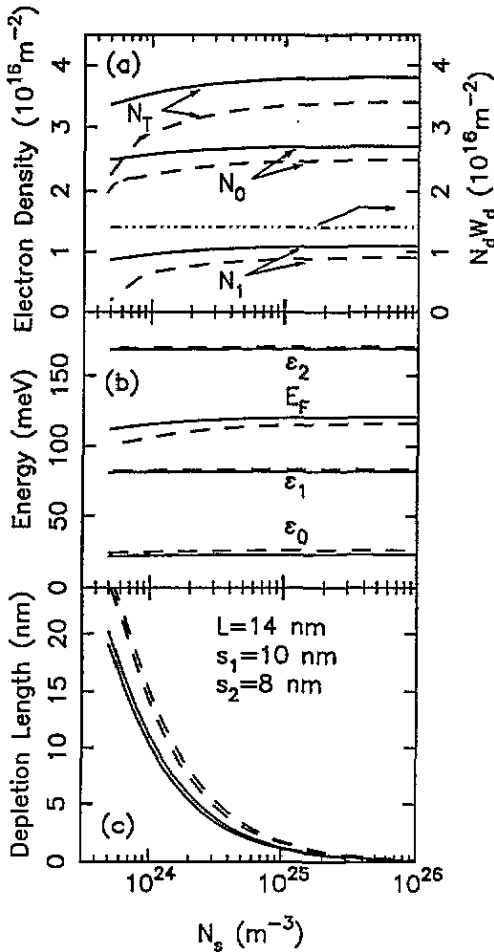


Figure 8. The dependence of the electronic properties on the concentration of the modulation-doped donor. The thinner curve shows the result of $N_d W_d$. The other lines are as in figure 5. $N_a = 2 \times 10^{20} \text{m}^{-3}$, $W_d = 2 \text{nm}$ and $N_d = 7 \times 10^{24} \text{m}^{-3}$.

Comparing our theoretical results with the experimental data reported recently [25] for the SQW without δ doping, (1) our results exhibit the correct dependence on the width of the quantum well of the total electron density, (2) when the width of the quantum well is around $L \sim 10 \text{nm} = 100 \text{\AA}$ the subband $n = 1$ is occupied by electrons, which was confirmed by the mobility measurements reported in [25] and (3) our results for the total electron density ($N_T \sim 10^{16} \text{m}^{-2}$) agree with the experimental data for the corresponding growth parameters. Quantitatively, the total electron densities obtained from our self-consistent calculation are smaller than those reported in [25] when $L < 10 \text{nm}$. It may be noted that in our calculations the conduction band discontinuity (U_0) between materials GaAs and AlGaAs is obtained from using equation (4), which leads to $U_0 \approx 203 \text{meV}$ at $c = 27\%$, a somewhat smaller value than $U_0 = 270 \text{meV}$ used in the calculations in [25]. Further, for the electron density in the different electronic subbands our self-consistent calculation gives slightly different results to those reported in [25], e.g., our result (figure 5(a)) shows that the electron density for the lowest subband ($n = 0$) decreases slightly with increasing width

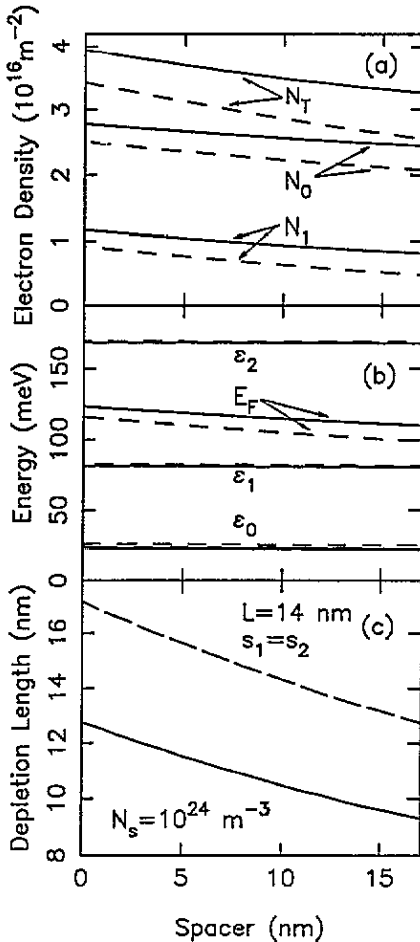


Figure 9. The dependence of the electronic properties on the symmetric spacers $s_1 = s_2$ for the fixed N_s and L . N_a , N_d and W_d are the same as in figure 8. The lines are as in figure 5.

of quantum well when the excited states ($n = 1$) are occupied in contrast with the rather marked decrease observed in [25]. Most published experimental data [16, 17, 26] on the electronic states of the δ -doped SQW structures were obtained by photoluminescence (PL) and photoluminescence excitation (PLE) spectroscopy as well as C - V profiles. In figure 5(b) our results for the δ -doped quantum well showed that the Fermi energy measured from the minimum of the conduction band edge in the GaAs layer decreases with increasing width of the quantum well layer, which agrees with the experimental result reported in [26] where the Fermi energy of the Si δ -doped quantum well was measured by using PL spectra with the thickness of the well layer varying from 5 to 20 nm. Our result for the profile of the confinement potential energy in a δ -doped SQW structure (see figures 2–4) did not show the structure expected in [26]: the electronic subband is located in the potential well caused by δ doping (see figure 3(a) in [26]). This is because (1) the actual conduction band bending has been included within our calculations and (2) we used a relatively small width of QW $L < 22$ nm. The larger the well width is, the stronger the influence of the δ doping will be, and consequently for a large enough L the electronic state will be in the potential well

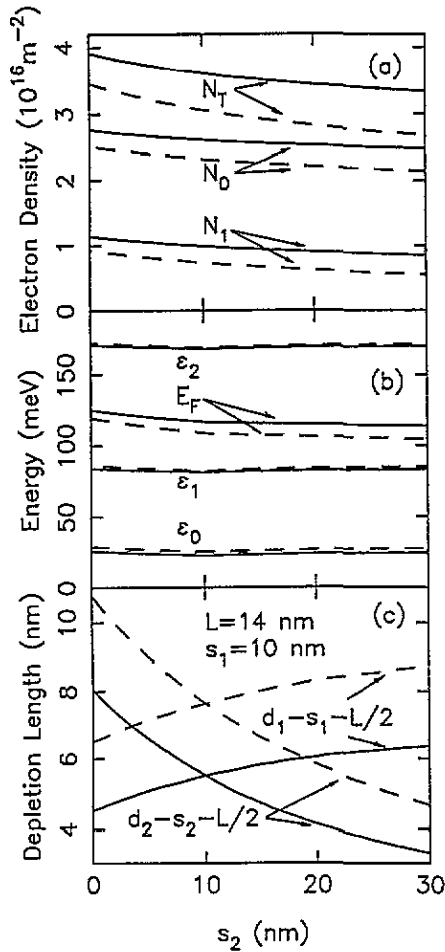


Figure 10. The dependence of the electronic properties on the spacer s_2 for fixed s_1 , L and $N_s = 2 \times 10^{24} \text{ m}^{-3}$. N_a , N_d and W_d are the same as in figure 8, and the lines are as in figure 5.

caused by δ doping.

4. Summary and conclusions

In this paper we have developed a simple self-consistent calculation on the electronic structure of Si δ -doped $\text{Al}_c\text{Ga}_{1-c}\text{As}-\text{GaAs}-\text{Al}_c\text{Ga}_{1-c}\text{As}$ single quantum wells at zero temperature. This model is a generalization of the self-consistent calculation proposed by Hurkx and van Haeringen in [8] in calculating the electronic states of the heterojunctions. In the calculations the inputs are (i) known material properties, such as effective electron masses, conduction band discontinuity, dielectric constant and donor binding energy and (ii) growth parameters, such as concentrations of the acceptor and modulation-doped donor dopants, spacer distances, Al content and concentration and thickness of the δ -doped layer. As outputs our calculation gives (1) the confinement potential, (2) the energies and the wavefunctions of the electronic subbands, (3) the electron distribution function along the

direction perpendicular to the interfaces of the two materials of GaAs and AlGaAs, (4) the depletion lengths, (5) the total sheet electron density and the electron densities in the occupied electronic subbands and (6) the Fermi energy measured from the minimum of the conduction band edge of GaAs for the δ -doped SQW. We have included the fact that the electron effective mass in GaAs differs from that in AlGaAs in our self-consistent calculation. Our model can also be applied to the situation with asymmetric modulation doping, i.e., to the case of $s_1 \neq s_2$. We studied the influence of the width of the quantum well, the selectively doped donor density, the spacer distances and the presence of a δ -doped layer in the well layer on the electronic structure of the SQW systems. Further, the results obtained from our theoretical calculations were compared with those obtained from experimental measurements. Our conclusions are summarized as follows.

In our model calculations the interesting physical quantities are obtained from known material properties and growth parameters only. Increasing width of the quantum well leads to a larger total electron density and to the occupation by electrons of the higher electronic subbands. A larger modulation-doped donor concentration and/or a smaller spacer distance result in a larger total electron density in an SQW structure, which is similar to the case of selectively doped AlGaAs/GaAs heterojunctions. In the single quantum well systems, the electronic subband energies are mainly determined by the width of the well layer and depend weakly on the modulation and δ doping.

The presence of a δ -doped layer in the middle of the quantum well layer results in (i) an extra confinement potential which is induced mainly by the Coulomb interaction and (ii) smaller depletion lengths in the modulation-doped AlGaAs layers. In the presence of this extra confinement potential energy, (i) the total confinement potential energy will be lowered in referring to the Fermi level and (ii) the separation between the energy of the occupied electronic subbands and the Fermi energy will be enhanced, and consequently a larger total electron density as well as larger electron densities in the occupied electronic subbands can be obtained. The smaller depletion lengths in a δ -doped SQW imply a non-linear increase in the total electron density with increasing concentration and thickness of the δ -doped layer. In our model calculations on the δ -doped SQW we assumed that all the δ -doped donors are ionized, which leads to a relatively weaker dependence of the total electron density on modulation doping, compared to the results obtained for the conventional SQWs. For the case of heavy modulation doping, the total electron density per unit area in an SQW with and without δ doping depends very little on the concentration of the modulation-doped donor, and the total number of ionized donors in AlGaAs regimes is roughly a constant given by $N_T - N_d W_d$.

The inclusion of different effective electron masses in the different materials leads to a slightly smaller total electron density than that obtained from taking $m^*(z) = m_0^*$. The depletion lengths obtained from the calculations are useful to guide device design and for further calculations regarding the impurity distributions, e.g., to the calculation of electronic mobility.

The results obtained from our self-consistent calculations agree with those obtained from the experimental measurements. For example, our theoretical results exhibit a correct dependence of the total electron density and the Fermi energy on well width and describe correctly the occupation by electrons of the electronic subbands.

Acknowledgments

This research has been carried out on behalf of the Harry Triguboff AM Research Syndicate.

Discussions with Dr M P Das, Dr C Jagadish and Dr A A Allerman are gratefully acknowledged.

References

- [1] Mimura T, Hiyamizu S, Fujii T and Nanbu K 1980 *Japan J. Appl. Phys.* **19** L225
- [2] See, e.g.,
Ferry D K (ed) 1985 *Gallium Arsenide Technology* (Indianapolis, IN: Sams)
- [3] See, e.g.,
Prange R E and Girvin S M (ed) 1987 *The Quantum Hall Effect* (New York: Springer)
- [4] Kastalsky A, Peeters F M, Chan W K, Florez L T and Harbison J P 1991 *Appl. Phys. Lett.* **59** 1708
Xu W, Peeters F M and Devreese J T 1993 *J. Phys.: Condens. Matter* **5** 2307; 1993 *Phys. Rev. B* **48** 1562
- [5] Ando T 1982 *J. Phys. Soc. Japan* **51** 3893, 3900
- [6] Stern F and Das Sarma S 1984 *Phys. Rev. B* **30** 840
- [7] Hihara H and Hamaguchi C 1985 *Solid State Commun.* **54** 485
Fletcher R, Zaremba E, D'Iorio M, Foxon C T and Harris J J 1990 *Phys. Rev. B* **41** 10649
- [8] Hurkx G A M and van Haeringen W 1985 *J. Phys. C: Solid State Phys.* **18** S617
- [9] Koenraad P M, Heessels A C L, Blom F A P, Perenboom J A A J and Wolter J H 1993 *Physica B* **184** 221
- [10] Inoue K, Sakaki H, Yoshino J and Hotta T 1985 *J. Appl. Phys.* **58** 4277
- [11] Kim T W, Lee J I, Kang K N, Lee K-S, Yoo K-H and Ihm G 1992 *J. Phys.: Condens. Matter* **4** 5763
- [12] Hamaguchi C, Miyatsuji K and Hihara H 1984 *Japan J. Appl. Phys.* **23** L132
- [13] Simserides C D and Triberis G P 1993 *J. Phys.: Condens. Matter* **5** 6437
- [14] Marmorosk I K and Das Sarma S 1993 *Phys. Rev. B* **48** 1544
- [15] Sakaki H 1982 *Japan J. Appl. Phys.* **21** L381
- [16] Schubert E F 1990 *Surf. Sci.* **228** 240
Wagner J, Fischer A and Ploog K 1990 *Phys. Rev. B* **42** 7280
Mendonca C A C, Scolfaro L M R, Oliveira J B B, Plentz F, Micovic M, Leite J R and Meneses E A 1992
Superlatt. Microstruct. **12** 257
- [17] Ke M L, Rimmer J S, Hamilton B, Evans J H, Missous M, Singer K E and Zalm P 1992 *Phys. Rev. B* **45** 14114
Shibli S M, Scolfaro L M R, Leite J R, Mendonca C A C, Plentz F and Meneses E A 1992 *Appl. Phys. Lett.* **60** 2895
- [18] Seeger K 1982 *Semiconductor Physics (An Introduction)* (Berlin: Springer) p 39
- [19] Lee H J, Juravel L Y, Wolley J C and Spring Thorpe A J 1980 *Phys. Rev. B* **21** 659
- [20] Kim T W, Lee J I, Kang K N, Lee K-S and Yoo K-H 1991 *Phys. Rev. B* **44** 12891
- [21] Kohn W and Sham L J 1965 *Phys. Rev.* **140** A1133
- [22] Jones R O and Gunnarsson O 1989 *Rev. Mod. Phys.* **61** 689
- [23] Hedin L and Lundqvist B I 1971 *J. Phys. C: Solid State Phys.* **4** 2064
- [24] Koonin S E 1986 *Computational Physics* (Reading, MA: Addison-Wesley)
- [25] Inoue K and Matsuno T 1993 *Phys. Rev. B* **47** 3771
- [26] Shih Y C and Streetman B G 1991 *Appl. Phys. Lett.* **59** 1344